Stem Cell Reports
Report

OPEN ACCESS

JAK/STAT-1 Signaling Is Required for Reserve Intestinal Stem Cell Activation during Intestinal Regeneration Following Acute Inflammation

Camilla A. Richmond,[1,3,*] Hannah Rickner,[2] Manasvi S. Shah,[2] Tracy Ediger,[1,3] Luke Deary,[2] Fanny Zhou,[2] Alessio Tovaglieri,[2] Diana L. Carlone,[2,3] and David T. Breault[2,3,4]

[1]Division of Gastroenterology
[2]Division of Endocrinology
Boston Children's Hospital, 300 Longwood Avenue, Boston, MA 02115, USA
[3]Department of Pediatrics, Harvard Medical School, Boston, MA 02115, USA
[4]Harvard Stem Cell Institute, Cambridge, MA 02138, USA
*Correspondence: camilla.richmond@childrens.harvard.edu
https://doi.org/10.1016/j.stemcr.2017.11.015

SUMMARY

The intestinal epithelium serves as an essential barrier to the outside world and is maintained by functionally distinct populations of rapidly cycling intestinal stem cells (CBC ISCs) and slowly cycling, reserve ISCs (r-ISCs). Because disruptions in the epithelial barrier can result from pathological activation of the immune system, we sought to investigate the impact of inflammation on ISC behavior during the regenerative response. In a murine model of αCD3 antibody-induced small-intestinal inflammation, r-ISCs proved highly resistant to injury, while CBC ISCs underwent apoptosis. Moreover, r-ISCs were induced to proliferate and functionally contribute to intestinal regeneration. Further analysis revealed that the inflammatory cytokines interferon gamma and tumor necrosis factor alpha led to r-ISC activation in enteroid culture, which could be blocked by the JAK/STAT inhibitor, tofacitinib. These results highlight an important role for r-ISCs in response to acute intestinal inflammation and show that JAK/STAT-1 signaling is required for the r-ISC regenerative response.

INTRODUCTION

The intestinal epithelium is a rapidly self-renewing tissue that plays an essential role in maintaining the balance between selective absorption and maintenance of barrier function. This balance is fundamentally disrupted in conditions such as inflammatory bowel disease (IBD), where immune dysregulation leads to breakdown of the epithelial barrier yielding mucosal ulcerations, malabsorption, and chronic systemic illness. While current efforts are focused on modulating the immune dysregulation inherent to IBD, the mechanisms underlying epithelial repair and restitution remain understudied and may lend insight into alternative approaches to the treatment of IBD.

The histopathologic feature of crypt branching, seen in IBD, results from crypt fission in response to crypt loss, and is likely associated with activation of intestinal stem cells (ISCs) and progenitor cells in the crypt (Jevon and Madhur, 2010). Two functionally distinct populations of ISCs are responsible for maintaining the epithelium: rapidly cycling crypt base columnar (CBC) ISCs, marked by *Lgr5* (Barker et al., 2007), and slowly cycling, reserve stem cells (r-ISCs) located in the "+4" supra-Paneth cell position and marked by telomerase (*mTert*) and other markers (Gracz et al., 2010; Montgomery et al., 2011; Takeda et al., 2011). Although CBC ISCs play an important role in daily intestinal maintenance, they are highly sensitive to injury, whereas r-ISCs are highly resistant to injury and contribute to the intestinal lineage during regeneration (Goodell et al., 2015; Richmond et al., 2015). What role r-ISCs play in response to inflammatory insults and what factors regulate their response have not yet been explored.

The role of cytokines and their downstream signaling pathways in the pathophysiology of IBD has been well studied with a primary focus on their regulation of immune function (Wittkopf et al., 2014). The JAK/STAT signaling pathway has been implicated in the regulation of the immune inflammatory response (Neurath, 2014; Wittkopf et al., 2014) and is activated in response to interferon-γ (IFN-γ) and tumor necrosis factor alpha (TNF-α), two key downstream inflammatory mediators of IBD pathogenesis. Whether this pathway also regulates the ISC response to inflammation, and thus epithelial regeneration following injury, remains unknown. Here, we report that in response to acute intestinal inflammation, r-ISCs are activated to enter the cell cycle, undergo JAK/STAT-1 activation, and functionally contribute to epithelial restitution.

RESULTS

Anti-CD3 Antibody Treatment Leads to Intestinal Injury Followed by Rapid Recovery

To investigate how ISCs respond to inflammation, we utilized a previously established model of T cell-mediated small-intestinal inflammation induced by administration of anti-CD3 antibody (αCD3) (Ferran et al., 1990). αCD3 leads to T cell activation, which results in an acute,

This is an open access article under the CC BY-NC-ND license (http://creativecommons.org/licenses/by-nc-nd/4.0/).

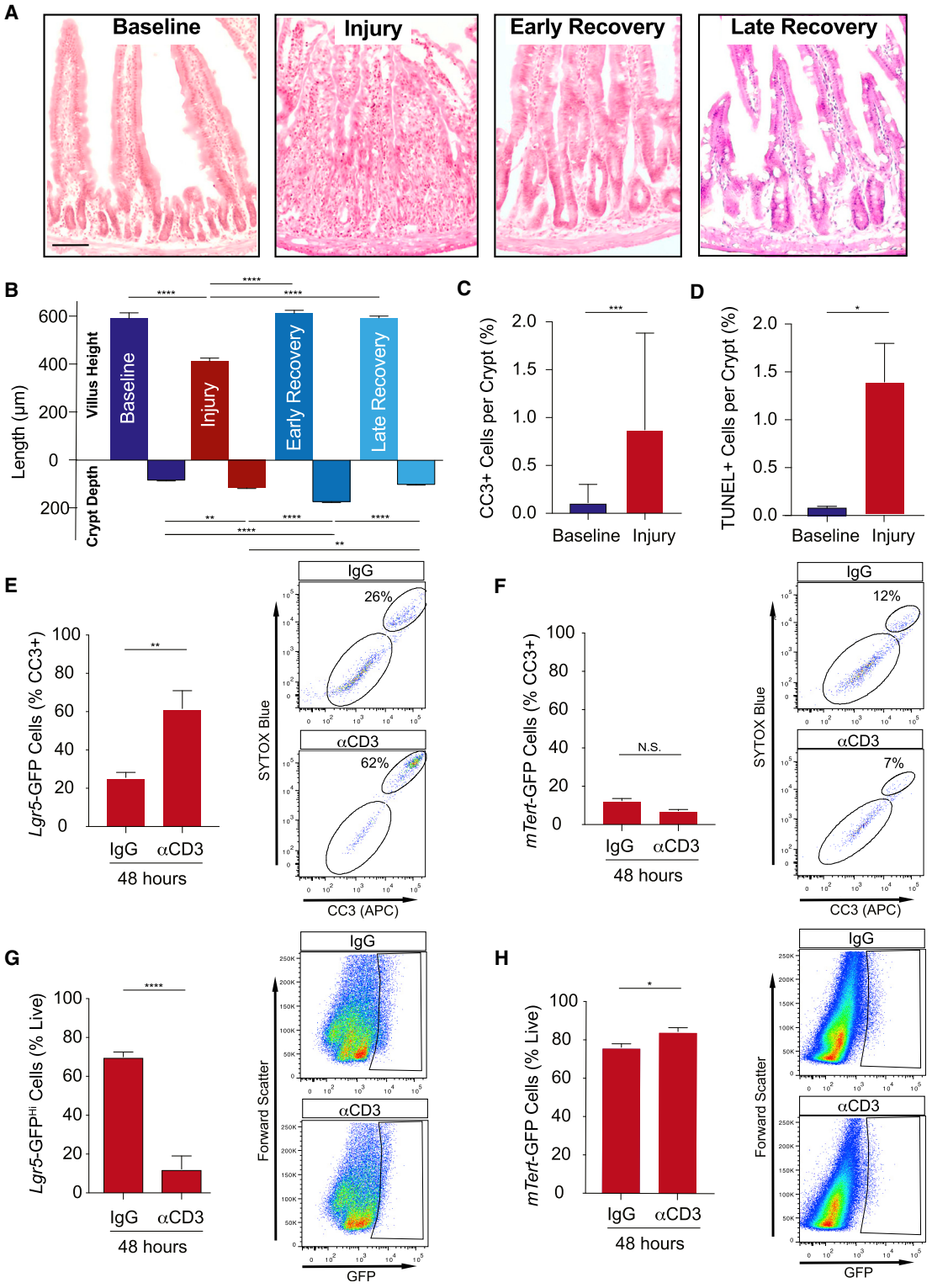

Figure 1. αCD3 Leads to Epithelial Injury and CBC Loss with Subsequent Recovery

(A) Representative H&E images of small intestine at baseline, injury, early recovery, and late recovery. Scale bar, 100 μm.

(B) Villus height and crypt depth (μm) following αCD3 compared with baseline. N = 2 mice/time point, 30/19, 83/83, 94/94, 147/147 total villus/crypt measurements counted.

(legend continued on next page)

self-limited "cytokine release syndrome" (CRS) of fever, enteritis, and diarrhea similar to an acute flare of IBD (Ferran et al., 1990). CRS is also associated with histomorphometric changes consisting of villus shortening, crypt degeneration, and cell death, mimicking IBD-associated small-intestinal pathology (Radojevic et al., 1999). Adult mice received a single intraperitoneal injection of αCD3 and the proximal small intestines were examined at baseline (day 0), peak injury (day 2), early (day 4), and late (day 6–7) recovery. Consistent with findings from other groups (Radojevic et al., 1999), we observed moderate to severe histological abnormalities at the peak of injury, with near normalization of histology by late recovery, underscoring the enormous regenerative capacity of this tissue (Figure 1A). Compared with baseline, mice treated with αCD3 showed decreased villus height and body weight at the peak of injury, followed by expansion of the crypt compartment during early recovery, and near resolution by the late recovery phase (Figures 1A, 1B, S1A, and S1B). The expansion of the crypt compartment, where ISCs reside, raised the possibility that ISCs sensed intestinal damage and initiated a regenerative response.

R-ISCs Are Resistant to Inflammation-Induced Apoptosis

Given the tissue damage caused by αCD3 (Figure 1A, injury), we anticipated a general increase in crypt cell death at the peak of injury. Using cleaved caspase-3 (CC3) as a marker for apoptosis, we analyzed the number of $CC3^+$ crypt cells at various time points during the 7-day experiment. As anticipated, evaluation of more than 10,000 crypts showed that the overall number of $CC3^+$ crypt cells increased 9-fold at the peak of injury (48 hr) with a subsequent gradual return to baseline levels (Figures 1C, S1C, and S1E). These findings were then independently confirmed by TUNEL staining (Figures 1D, S1D, and S1F). To analyze the rate of ISC apoptosis at the peak of injury, we utilized the previously validated *mTert*-GFP mouse model, as a reporter of r-ISCs (Breault et al., 2008), and the *Lgr5*-GFP mouse model, as a reporter of CBC ISCs (Barker et al., 2007). We scored small-intestinal crypt sections co-stained for GFP and CC3 from mice treated with either αCD3 antibody or isotype control IgG. Unsurprisingly, given the level of epithelial damage (Figure 1A, injury), immunofluorescent analysis of CBC ISCs at the peak of injury showed a dramatic increase in the number of co-positive *Lgr5*-GFP^+ $CC3^+$ cells (from 0.7% to 16%), a 22-fold increase compared with controls (Figure S1G). These findings were confirmed using flow cytometric analysis of CC3 at the same time point, which showed that ~60% of CBC ISCs were $CC3^+$, underscoring their vulnerability to inflammatory injury (Figure 1E). In contrast, analysis of CC3 in r-ISCs at the peak of injury revealed no apoptosis (0 of 39 *mTert*-GFP^+ cells) by immunofluorescence and no change in the number of *mTert*-GFP^+ $CC3^+$ co-positive cells by flow cytometric analysis (Figure 1F), indicating that these cells are resistant to inflammation-induced injury. Consistent with the above, there was a significant decrease in the number of surviving $Lgr5^{hi}$ ISCs (Figures 1G and S1H) while the number of viable *mTert* r-ISCs showed a modest increase following αCD3 treatment (Figures 1H and S1I). Together, these data demonstrate that r-ISCs are highly resistant to inflammation while CBC ISCs are highly sensitive and underscore the differential response of the two ISC populations to intestinal injury.

R-ISCs Are Activated to Enter the Cell Cycle in Response to Inflammation

Previously, our lab and others have shown that r-ISCs function as a reserve stem cell population that can be activated in response to intestinal damage (Richmond et al., 2015; Tian et al., 2011). Therefore, we next examined whether *mTert*-GFP^+ r-ISCs were activated in response to αCD3-induced intestinal injury. Analysis of crypt sections revealed a significant increase (2.3-fold) in the number of *mTert*-GFP^+ cells during the early recovery phase compared with baseline (Figure 2A), suggesting a possible role for these cells in the recovery following inflammatory damage. We next investigated if the increase in *mTert*-GFP^+ cell number was due to enhanced proliferation within this normally quiescent population (Breault et al., 2008). Immunofluorescent analysis of intestinal crypt sections revealed that ~30% of *mTert*-GFP^+ cells in αCD3-treated mice were $Ki67^+$ (a marker of proliferation) at the early stage of recovery, compared with only ~2% in controls (Figures 2B and S2A). A similar increase in proliferation was observed in *mTert*-GFP mice administered ethynyl deoxyuridine (EdU)

(C) Crypt cells expressing cleaved caspase-3 (CC3) at baseline (N = 20) and injury (N = 9).
(D) Crypt cells expressing TUNEL at baseline (N = 4) and injury (N = 7).
(E) *Lgr5*-$GFP^+CC3^+CD45^-PI^-$ cells 48 hr after control IgG (N = 3) and αCD3 (N = 3).
(F) *mTert*-$GFP^+CC3^+CD45^-PI^-$ cells 48 hr after control IgG (N = 3) or αCD3 (N = 3).
(G) Live *Lgr5*-GFP^{hi} cells 48 hr after control IgG (N = 3) or αCD3 (N = 3).
(H) Live *mTert*-GFP cells 48 hr after control IgG (N = 3) or αCD3 (N = 3).
Error bars indicate the SEM. *$p < 0.05$, **$p < 0.01$, ***$p < 0.001$, ****$p < 0.0001$, n.s., not significant. Representative flow cytometry plots shown.

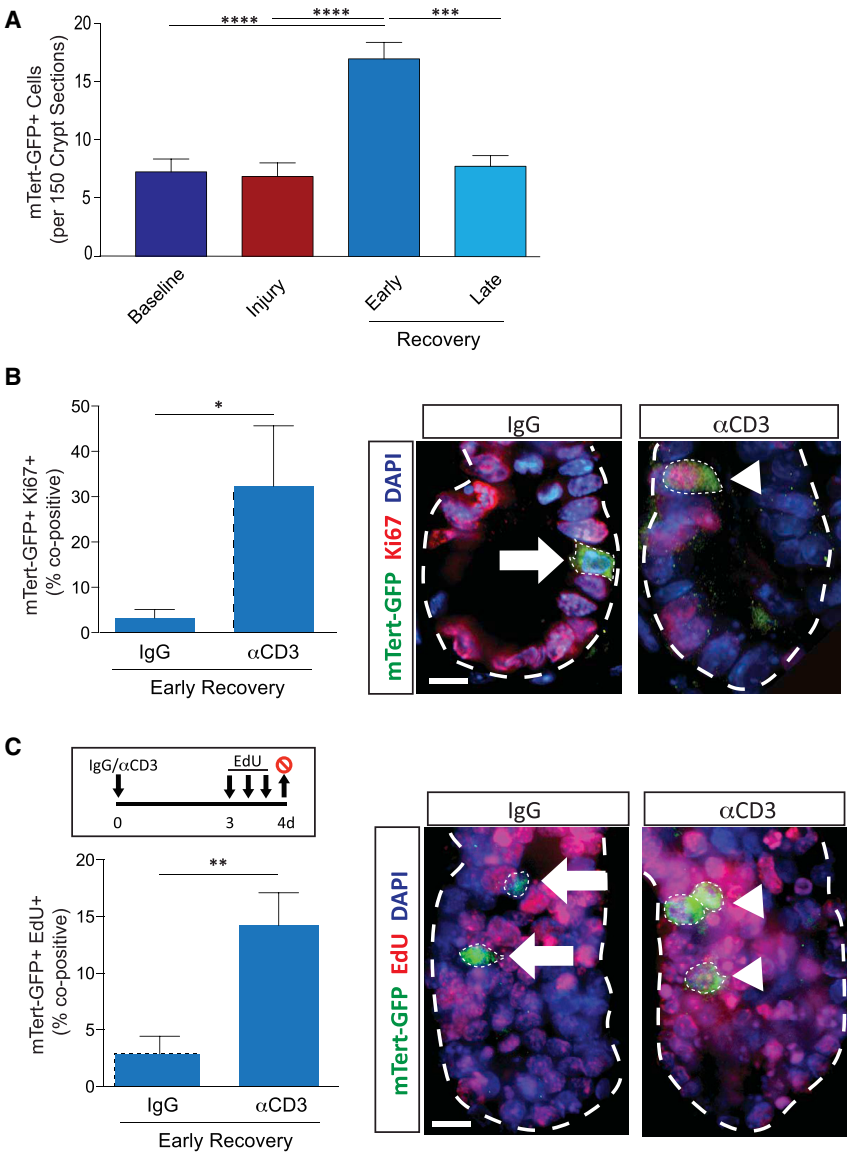

Figure 2. R-ISC Numbers Increase and Enter the Cell Cycle following αCD3

(A) *mTert*-GFP$^+$ crypt cells per 150 crypt sections at baseline, injury, early recovery, and late recovery. N = 2 mice/time point, 18, 21, 20, and 9 sections counted.

(B) *mTert*-GFP$^+$ crypt cells co-expressing Ki67 in control IgG and αCD3-treated mice at early recovery. Representative optical sections from control IgG- (N = 8) and αCD3-treated (N = 4) mice showing cycling (arrowhead) and quiescent (arrow) *mTert*-GFP$^+$ cells in merged, DAPI, *mTert*-GFP, and Ki67 channels.

(C) *mTert*-GFP$^+$ cells co-expressing EdU in isolated crypts from control IgG- (N = 3) and αCD3-treated (N = 3) mice at early recovery. Representative optical sections showing quiescent *mTert*-GFP$^+$ cells (arrow) in control IgG and cycling *mTert*-GFP$^+$ cells in αCD3-treated (arrowhead) crypts in merged DAPI, *mTert*-GFP, and EdU (Click-iT) channels.

Error bars indicate the SEM. *p < 0.05, **p < 0.01, ***p < 0.001, ****p < 0.0001. Scale bar, 10 μm.

on day 3 following αCD3 treatment and then analyzed by 3D whole-mount crypt analysis on day 4. Analysis of 388 *mTert*-GFP$^+$ cells from 800 isolated crypts showed a significant increase in the number (3% →14%) of *mTert*-GFP$^+$ EdU$^+$ co-positive cells between control and αCD3-treated mice (Figures 2C and S2B). A more limited increase in cycling frequency was seen in the CBC ISC compartment during early recovery (Figure S2C), likely representing increased proliferation in cells that survived the inflammation or in those already replenished by the activated r-ISC population (Montgomery et al., 2011). Taken together, these data show that the marked increase in *mTert*-GFP$^+$ cells occurs through enhanced proliferation during the early recovery period in response to the inflammatory milieu.

Activated r-ISCs Contribute to Intestinal Regeneration Following Inflammation

To functionally assess whether r-ISCs that were activated in response to inflammation had the capacity to contribute to intestinal regeneration during the recovery phase, we performed lineage-tracing studies. For these experiments, we employed the previously validated tamoxifen-inducible *mTert*-CreER::R26R(LacZ) bigenic mouse model to mark r-ISCs (Montgomery et al., 2011). To ensure concordant expression of this model with mice expressing the *mTert*-GFP allele, we generated enteroids from trigenic *mTert*-GFP::*mTert*-CreER::R26R(LacZ) mice. Flow cytometric analysis of these enteroids revealed that the majority of LacZ$^+$ cells co-expressed GFP, confirming that the two mouse models label the same cell population

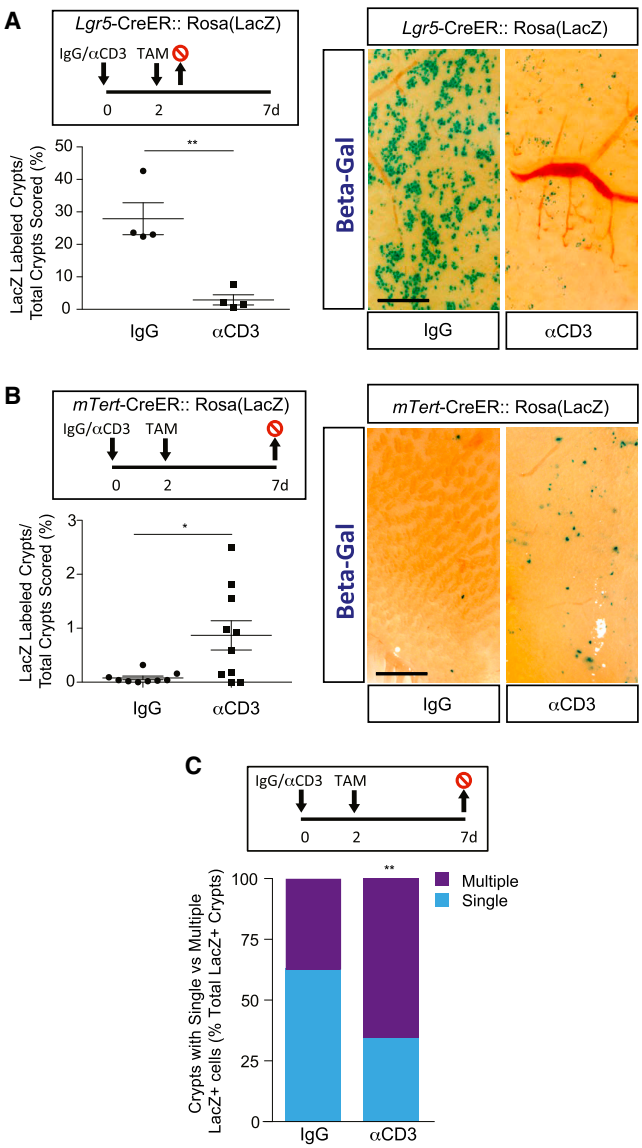

Figure 3. R-ISCs Show Increased Lineage Contribution Following αCD3 while the CBC Contribution Is Reduced

(A) Quantitative whole-mount analysis showing a decrease in the number of lineage-marked LacZ$^+$ crypts from *Lgr5*-Cre::R26R(LacZ) IgG- (N = 4) and αCD3-treated (N = 4) mice at injury. Representative whole mounts of β-gal$^+$ crypts.

(B) Quantitative whole-mount analysis showing increase in the number of lineage-marked LacZ$^+$ crypts from *mTert*-Cre::R26R(LacZ) IgG- (N = 9) and αCD3-treated (N = 10) mice during late recovery. Representative whole mounts of β-gal$^+$ crypts.

(C) Change in distribution of crypts with single and multiple *mTert*-LacZ$^+$ cells 7 days after IgG (N = 9 mice) or αCD3 (N = 10 mice) indicating an increase in the number of crypts with multiple cells following αCD3 treatment.

Error bars indicate the SEM. *$p < 0.05$, **$p < 0.01$. Scale bar, 1 mm.

(Figures S3A and S3B). Further analysis additionally confirmed a 6-fold enrichment of Cre expression in GFP$^+$ cells isolated by fluorescence-activated cell sorting compared with GFP$^-$ cells (Figure S3C). *Lgr5*-CreER::R26R(LacZ) bigenic mice were used to assess the response of CBC ISCs (Barker et al., 2007). Mice received either αCD3 or IgG at the initiation of the experiment followed by a single dose of tamoxifen at the peak of injury (day 2). Intestines were then harvested either 1 day later (day 3) to elucidate the immediate ISC response, or at the late recovery time point (day 7) to elucidate their regenerative contribution, and analyzed by quantitative whole-mount LacZ staining. When analyzed 1 day following the peak of injury, *Lgr5*-CreER::R26R(LacZ) mice revealed an 11-fold decrease in the total number of *Lgr5*-LacZ-marked crypts (Figure 3A), consistent with their increased rate of apoptosis in response to injury (Figures 1E and S1G). Analysis of *mTert*-CreER::R26R(LacZ) mice killed on day 3 showed no significant change in overall LacZ crypt labeling although there was a trend toward an increase at this early time point (Figure S3D). Analysis at the late recovery time point however revealed a 6-fold increase in the total number of *mTert*-LacZ-marked crypts (Figure 3B), highlighting their robust response to this regenerative pressure. Further analysis revealed that, after αCD3 treatment, the majority of these *mTert*-LacZ-labeled crypts contained multiple lineage-marked cells (Figure 3C), consistent with the increase in r-ISC proliferation observed above (Figures 2B and 2C). By the late recovery time point, the number of *Lgr5*-LacZ-marked crypts had rebounded to control levels (Figure S3E), suggesting that CBC ISCs also support the regenerative recovery once their population is replenished. Taken together, these data confirm that r-ISCs, activated in response to inflammatory injury, contribute to the regenerative response, followed by a secondary wave of CBC ISC activation to support full epithelial restitution.

Finally, to rule out that the increase in labeled crypt cells did not result from activation of the *mTert* promoter, *mTert*-CreER::R26R(LacZ) mice were pre-treated with tamoxifen to mark the r-ISC population during a non-inflamed baseline state. Because of its long biological half-life (Robinson et al., 1991), tamoxifen was allowed to wash out for 10 days before mice were administered either αCD3 or IgG, and intestines were analyzed 4 days later, during the early recovery phase. Quantitative whole-mount LacZ analysis revealed an increase (11-fold) in the number of crypts containing multiple LacZ$^+$ cells (Figure S3F), likely due to division of cells labeled prior to injury and consistent with activation of the reserve ISC population. These results support our above findings that r-ISCs are activated to enter the cell cycle in response to inflammation and contribute to the regenerative response.

Interferon-γ and Tumor Necrosis Factor Alpha Activate r-ISCs *In Vitro*

The primary cytokines released in response to αCD3 administration include IFN-γ and TNF-α, important mediators of IBD in humans (Ferran et al., 1991; Musch et al., 2002). To investigate whether these cytokines mediated the inflammation-induced activation of r-ISCs, we turned to the enteroid culture system (Sato et al., 2009). Initially, we confirmed that enteroids could respond to exogenous cytokine treatment. Mature enteroids were treated with IFN-γ (5 ng/mL) or vehicle and assayed for induction of downstream target genes (*Irf1*, *Stat-1*, *Nfkb*, and *Ccnd1*) (Cheon and Stark, 2009; Rauch et al., 2013). qRT-PCR analysis revealed robust induction of each gene within 4 hr (Figure S4A), indicating that enteroids can respond to exogenous cytokine stimulation. We then derived enteroids from *mTert*-GFP mice and cultured them in the presence of IFN-γ or vehicle (PBS). Flow cytometric analysis after 48 hr of treatment revealed a ~2-fold increase in GFP$^+$ cells following IFN-γ treatment compared with vehicle-treated controls (Figure 4A). In contrast, enteroids derived from *Lgr5*-GFP mice revealed a 67% decrease in *Lgr5*-GFP^{hi+} cells following IFN-γ treatment (Figure 4B). We also examined the effect of TNF-α (50 ng/mL) on *mTert*-GFP-derived enteroids and observed a similar increase in *mTert*-GFP$^+$ cells (Figure S4B). The increase in *mTert*-GFP$^+$ r-ISC cells in response to both IFN-γ and TNF-α, the two major cytokines involved in the αCD3-induced cytokine storm and in human IBD, suggests that activation of r-ISCs *in vivo* may result from direct immune-epithelial cell crosstalk.

JAK/STAT-1 Pathway Activates r-ISCs in Response to Inflammation

Since IFN-γ and TNF-α are known to mediate their effects through JAK/STAT signaling (Li, 2008; Rauch et al., 2013), we next investigated the role of this pathway *in vivo*, using intestinal crypt sections from mice at early and late recovery time points following αCD3 or IgG administration. Immunofluorescent analysis for the active form of STAT-1, phospho-STAT-1 (pSTAT-1), revealed no significant change in the total number of pSTAT-1$^+$ crypt cells (Figure S4C). However, specific analysis of *mTert*-GFP$^+$ cells revealed a dramatic increase in the percentage of *mTert*-GFP$^+$ pSTAT-1$^+$ co-labeled cells during the early recovery time point, which returned to baseline levels by the late recovery time point (Figures 4C and S4D). In contrast, analysis of co-expression of *mTert*-GFP$^+$ cells with either pSTAT-5 or pSTAT-3, both previously suggested to play a role in the intestinal epithelial response to inflammation (Lindemans et al., 2015; Matthews et al., 2011), revealed a marked decrease in pSTAT-5 co-expression at the early recovery time point (Figure S4E), and no *mTert*-GFP$^+$ cells (0 of 181) that co-expressed pSTAT-3. In addition, no significant changes in pSTAT-1 co-expression were detected in CBC ISCs *in vivo* (Figure S4F), reinforcing the differential mechanisms involved in the response of r-ISCs and CBC ISCs to inflammation. These data indicate that JAK/STAT-1 signaling is activated by inflammation during the r-ISC regenerative response.

Finally, to investigate if JAK/STAT-1 signaling was required for the activation of r-ISCs during inflammation, we pre-treated enteroid cultures derived from *mTert*-GFP mice with tofacitinib (TOFA), a pan-JAK/STAT inhibitor, recently approved by the US Food and Drug Administration for the treatment of ulcerative colitis (Sandborn et al., 2014), prior to administration of IFN-γ. Inhibition of JAK/STAT signaling with TOFA completely blocked the IFN-γ-driven induction in r-ISC number otherwise seen after treatment, yielding comparable numbers as vehicle-treated controls (Figure 4D). Taken together, these data indicate that JAK/STAT-1 signaling activates r-ISCs following inflammatory injury and underlies their regenerative response.

DISCUSSION

Here, we report the results of *in vitro* and *in vivo* analyses examining the effects of inflammation on reserve and CBC ISCs, including their relative contribution to intestinal regeneration. Our findings show that small-intestinal inflammation induced by αCD3 leads to (1) marked tissue damage associated with an increase in apoptosis in CBC ISCs but not r-ISCs, (2) an increase in r-ISC number resulting from their activation to enter the cell cycle, (3) an increase in r-ISC lineage contribution during the regenerative response, and (4) activation of JAK/STAT-1 signaling within r-ISCs. These results are in contrast to the response of CBC ISCs, which show a reduced regenerative capacity immediately following the injury. This differential response is further substantiated by an increasing body of literature supporting the notion that pathways important for regulation of ISCs in response to tissue injury, both in mammals and *Drosophila*, are distinct from those that regulate tissue maintenance (Biteau et al., 2011).

Our findings confirm previously reported structural changes in the small intestine following αCD3 treatment, including a reduction in villus height followed by an increase in the average crypt depth. Utilizing the major cytokines (IFN-γ, TNF-α) released during αCD3 treatment *in vivo* (Ferran et al., 1990), we developed an *in vitro* system to model the epithelial response to inflammation. This model showed an increase in the number of r-ISCs in response to these cytokines, providing a potential link between immune cells and epithelial stem cells. Our *in vitro* analysis also revealed activation of the canonical JAK/STAT-1

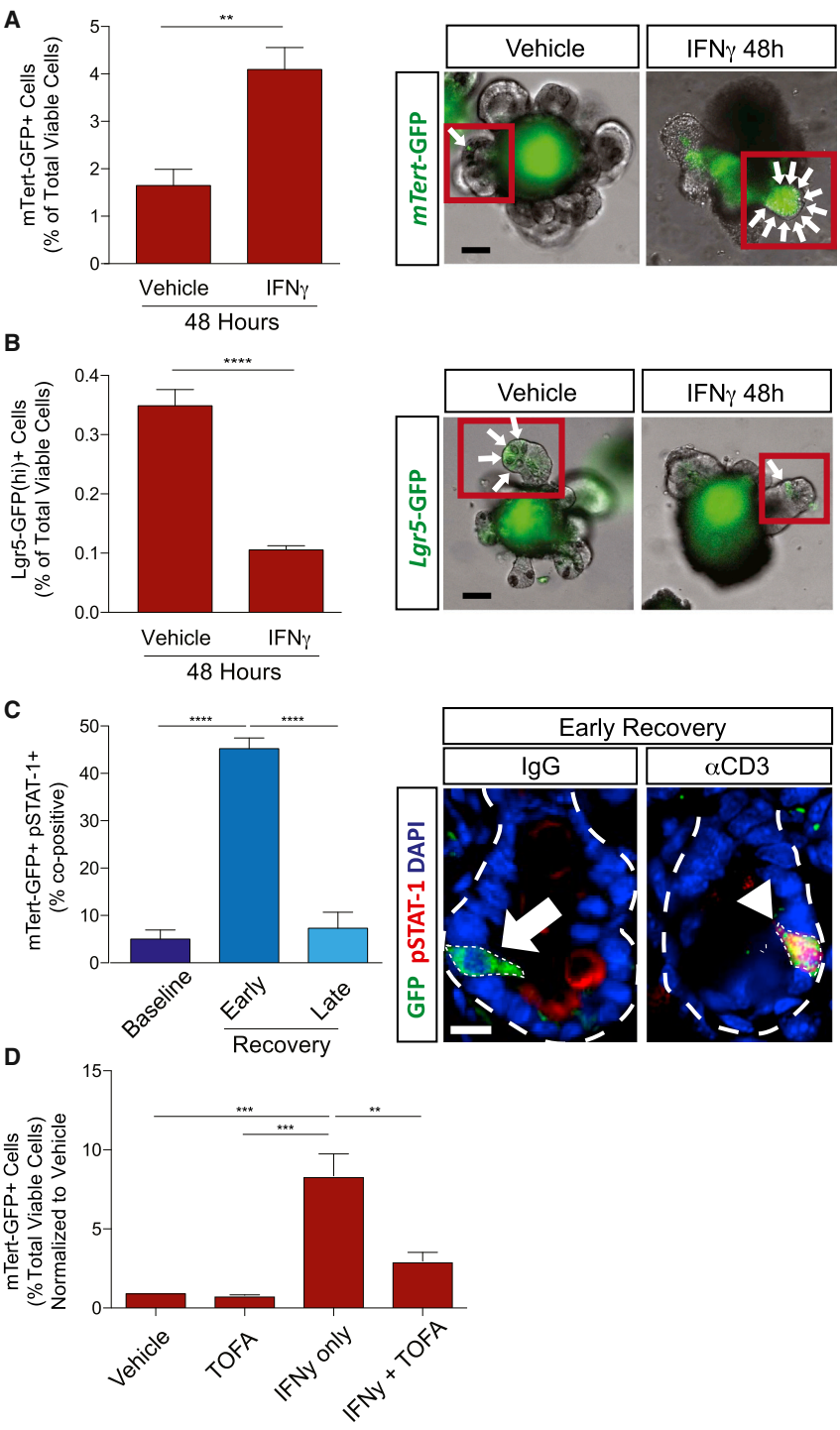

Figure 4. Cytokines Induce R-ISCs via JAK/STAT-1

(A) Live *mTert*-GFP$^+$ cells from vehicle (PBS)- and IFN-γ-treated enteroid cultures after 48 hr. Representative images of *mTert*-GFP enteroid cultures 48 hr after vehicle or IFN-γ. Arrows identify *mTert*-GFP$^+$ cells. Enteroid lines derived from N = 3 mice. Scale bar, 50 μm.

(B) Live *Lgr5*-GFP^{hi} cells from vehicle and IFN-γ-treated enteroid cultures after 48 hr. Representative images of *Lgr5*-GFP enteroid cultures 48 hr after vehicle or IFN-γ. Arrows identify *Lgr5*-GFP$^+$ cells. Enteroid lines derived from N = 3 mice. Scale bar, 50 μm.

(C) *mTert*-GFP$^+$ crypt cells that co-express pSTAT-1 at baseline (N = 7 mice), early recovery (N = 4 mice), and late recovery (N = 3 mice). Representative optical sections showing an *mTert*-GFP$^+$ pSTAT-1$^-$ cell (arrow) in IgG-treated and an *mTert*-GFP$^+$ pSTAT-1$^+$ cell (arrowhead) in αCD3-treated mice at early recovery in DAPI, *mTert*-GFP, and pSTAT-1 merged channels. Scale bar, 10 μm.

(D) Fold change in *mTert*-GFP$^+$ enteroid cells following treatment with vehicle, JAK/STAT-1 inhibitor tofacitinib (TOFA) only, IFN-γ only, and IFN-γ + TOFA. Enteroid lines derived from N = 3 mice.

Error bars indicate the SEM. $^{**}p < 0.01$, $^{***}p < 0.001$, $^{****}p < 0.0001$.

signaling pathway. To confirm this *in vivo*, we performed co-immunofluorescent analysis, which revealed that STAT-1 is the dominant pathway in r-ISCs. Given that both IFN-γ and TNF-α are traditionally considered to be "pro-inflammatory" cytokines that have a negative impact on intestinal function (Luissint et al., 2016), these data raise the possibility that specific cytokine signaling pathways may have differential effects on the epithelium in general, and on ISCs in particular.

Consistent with the above observation, although IFN-γ is generally considered to disrupt the intestinal epithelial barrier by blocking intestinal epithelial cell (IEC) proliferation

and increasing IEC apoptosis (Beaurepaire et al., 2009; Goretsky et al., 2012), it has more recently been reported to also support intestinal barrier function by stimulating the expression of interleukin-10 receptor on IECs (Kominsky et al., 2014). IFN-γ has also been found to attenuate tissue damage via upregulation of matrix metalloproteinases (Ma et al., 2001), modulation of prostaglandin E2 metabolism (Barrios-Rodiles and Chadee, 1998), and reduction in lymphocyte infiltration (Vermeire et al., 1997), all suggesting that it may have diverse and even paradoxical effects on distinct cell populations within the epithelium.

The epithelium can also produce cytokines itself that support wound healing after injury (Stadnyk, 1994). In *Drosophila*, stressed IECs produce cytokines, which can activate pro-mitogenic JAK/STAT signaling in an autocrine/paracrine fashion (Jiang et al., 2009; Zhou et al., 2013). Following tissue injury in mammals and in response to local cytokine production, IECs lose their cellular polarity and migrate to cover the wound in an attempt to maintain intestinal barrier function (Neurath, 2014; Sturm and Dignass, 2008). Termed "epithelial restitution," this process is regulated by cytokines (Dignass and Podolsky, 1993; Neurath, 2014) and is increasingly recognized as a critical component of mucosal healing following a flare of IBD. This process is driven by the proliferative crypt compartment and is tightly regulated (Neurath, 2014). Although STAT-3 and STAT-5 signaling have both been implicated in supporting wound healing, both in general and in CBC ISCs in particular (Gilbert et al., 2015; Lindemans et al., 2015), our work supports an important role for STAT-1 signaling in regulating the regenerative response of r-ISCs.

Although often associated with negative regulation of cell-cycle genes (Chin et al., 1996) and positive regulation of cleaved caspase-3 (Kumar et al., 1997), in this study, STAT-1 activation in r-ISCs was associated with entry into the cell cycle and prevention of apoptosis in response to inflammation. STAT-1 signaling is also required for production of nitric oxide during inflammation (Stempelj et al., 2007), and may, therefore, mediate IEC survival by helping to maintain mucosal integrity (McCafferty et al., 1997). In addition, JAK/STAT signaling positively regulates the Notch signaling pathway in ISCs, potentially facilitating the inter-conversion between r-ISCs and CBC ISCs and subsequent restitution of the CBC ISC population following tissue injury, thereby supporting epithelial wound healing (Pitsouli et al., 2009; Srinivasan et al., 2016).

Taken together, our results demonstrate that, in response to acute inflammation induced by αCD3, r-ISCs are activated to proliferate and functionally contribute to the subsequent regenerative response when CBC ISCs are initially lost or damaged. Mechanistically, this response requires, at least in part, the induction of JAK/STAT-1 signaling specifically within r-ISCs. This work raises important questions regarding how best to target inflammatory signaling pathways in order to optimally support the r-ISC regenerative response.

EXPERIMENTAL PROCEDURES

Detailed methods are available in Supplemental Information.

Statistical Analysis

Two-tailed Student's t test was used to compare groups of two- and one-way ANOVA with Bonferroni post hoc analysis to compare groups of three or more. Unless otherwise stated, means ± SEM are shown and N refers to the number of animals analyzed. Statistical significance was set at $p < 0.05$.

Study Approval

Animal procedures were approved by the BCH IACUC.

SUPPLEMENTAL INFORMATION

Supplemental Information includes Supplemental Experimental Procedures and four figures and can be found with this article online at https://doi.org/10.1016/j.stemcr.2017.11.015.

AUTHOR CONTRIBUTIONS

C.A.R., D.L.C., and D.T.B. designed the experiments, wrote and edited the manuscript. C.A.R. and D.B. analyzed the data. M.S.S. and H.R. performed the qRT-PCR. H.R., F.Z., and A.T. performed the enteroid experiments. C.A.R., H.R., M.S.S., and F.Z. performed the flow cytometry. C.A.R. and T.E. performed the lineage tracing experiments. C.A.R., H.R., T.E., and L.D. performed the IHC experiments.

ACKNOWLEDGMENTS

We thank members of the Breault laboratory and R. Montgomery. This research was supported by NIH 5K12HD5289610, K08 DK106562-01A1, BCH Office of Faculty Development Award, HDDC P&F Award (to C.A.R.), F32DK107108 (to M.S.S.), R01DK084056, the Timothy Murphy Fund, the IDDRC P30HD18655, and the HDDC P30DK034854 (to D.T.B.).

Received: October 13, 2016
Revised: November 16, 2017
Accepted: November 17, 2017
Published: December 21, 2017

REFERENCES

Barker, N., van Es, J.H., Kuipers, J., Kujala, P., van den Born, M., Cozijnsen, M., Haegebarth, A., Korving, J., Begthel, H., Peters, P.J., et al. (2007). Identification of stem cells in small intestine and colon by marker gene Lgr5. Nature *449*, 1003–1007.

Barrios-Rodiles, M., and Chadee, K. (1998). Novel regulation of cyclooxygenase-2 expression and prostaglandin E2 production by IFN-gamma in human macrophages. J. Immunol. *161*, 2441–2448.

Beaurepaire, C., Smyth, D., and McKay, D.M. (2009). Interferon-gamma regulation of intestinal epithelial permeability. J. Interferon Cytokine Res. *29*, 133–144.

Biteau, B., Hochmuth, C.E., and Jasper, H. (2011). Maintaining tissue homeostasis: dynamic control of somatic stem cell activity. Cell Stem Cell *9*, 402–411.

Breault, D.T., Min, I.M., Carlone, D.L., Farilla, L.G., Ambruzs, D.M., Henderson, D.E., Algra, S., Montgomery, R.K., Wagers, A.J., and Hole, N. (2008). Generation of mTert-GFP mice as a model to identify and study tissue progenitor cells. Proc. Natl. Acad. Sci. USA *105*, 10420–10425.

Cheon, H., and Stark, G.R. (2009). Unphosphorylated STAT-1 prolongs the expression of interferon-induced immune regulatory genes. Proc. Natl. Acad. Sci. USA *106*, 9373–9378.

Chin, Y.E., Kitagawa, M., Su, W.C., You, Z.H., Iwamoto, Y., and Fu, X.Y. (1996). Cell growth arrest and induction of cyclin-dependent kinase inhibitor p21 WAF1/CIP1 mediated by STAT-1. Science *272*, 719–722.

Dignass, A.U., and Podolsky, D.K. (1993). Cytokine modulation of intestinal epithelial cell restitution: central role of transforming growth factor beta. Gastroenterology *105*, 1323–1332.

Ferran, C., Sheehan, K., Dy, M., Schreiber, R., Merite, S., Landais, P., Noel, L.H., Grau, G., Bluestone, J., Bach, J.F., et al. (1990). Cytokine-related syndrome following injection of anti-CD3 monoclonal antibody: further evidence for transient in vivo T cell activation. Eur. J. Immunol. *20*, 509–515.

Ferran, C., Sheehan, K., Schreiber, R., Bach, J.F., and Chatenoud, L. (1991). Anti-TNF abrogates the cytokine-related anti-CD3 induced syndrome. Transplant. Proc. *23*, 849–850.

Gilbert, S., Nivarthi, H., Mayhew, C.N., Lo, Y.H., Noah, T.K., Vallance, J., Rülicke, T., Müller, M., Jegga, A.G., Tang, W., et al. (2015). Activated STAT5 confers resistance to intestinal injury by increasing intestinal stem cell proliferation and regeneration. Stem Cell Reports *4*, 209–225.

Goodell, M.A., Nguyen, H., and Shroyer, N. (2015). Somatic stem cell heterogeneity: diversity in the blood, skin and intestinal stem cell compartments. Nat. Rev. Mol. Cell Biol. *16*, 299–309.

Goretsky, T., Dirisina, R., Sinh, P., Mittal, N., Managlia, E., Williams, D.B., Posca, D., Ryu, H., Katzman, R.B., and Barrett, T.A. (2012). p53 mediates TNF-induced epithelial cell apoptosis in IBD. Am. J. Pathol. *181*, 1306–1315.

Gracz, A.D., Ramalingam, S., and Magness, S.T. (2010). Sox9-expression marks a subset of CD24-expressing small intestine epithelial stem cells that form organoids in vitro. Am. J. Physiol. Gastrointest. Liver Physiol. *298*, G590–G600.

Jevon, G.P., and Madhur, R. (2010). Endoscopic and histologic findings in pediatric inflammatory bowel disease. Gastroenterol. Hepatol. (N. Y.) *6*, 174–180.

Jiang, H., Patel, P.H., Kohlmaier, A., Grenley, M.O., McEwen, D.G., and Edgar, B.A. (2009). Cytokine/JAK/STAT signaling mediates regeneration and homeostasis in the *Drosophila* midgut. Cell *137*, 1343–1355.

Kominsky, D.J., Campbell, E.L., Ehrentraut, S.F., Wilson, K.E., Kelly, C.J., Glover, L.E., Collins, C.B., Bayless, A.J., Saeedi, B., Dobrinskikh, E., et al. (2014). IFN-gamma-mediated induction of an apical IL-10 receptor on polarized intestinal epithelia. J. Immunol. *192*, 1267–1276.

Kumar, A., Commane, M., Flickinger, T.W., Horvath, C.M., and Stark, G.R. (1997). Defective TNF-alpha-induced apoptosis in STAT-1-null cells due to low constitutive levels of caspases. Science *278*, 1630–1632.

Li, W.X. (2008). Canonical and non-canonical JAK-STAT signaling. Trends Cell Biol. *18*, 545–551.

Lindemans, C.A., Calafiore, M., Mertelsmann, A.M., O'Connor, M.H., Dudakov, J.A., Jenq, R.R., Velardi, E., Young, L.F., Smith, O.M., Lawrence, G., et al. (2015). Interleukin-22 promotes intestinal-stem-cell-mediated epithelial regeneration. Nature *528*, 560–564.

Luissint, A.C., Parkos, C.A., and Nusrat, A. (2016). Inflammation and the intestinal barrier: leukocyte-epithelial cell interactions, cell junction remodeling, and mucosal repair. Gastroenterology *151*, 616–632.

Ma, Z., Qin, H., and Benveniste, E.N. (2001). Transcriptional suppression of matrix metalloproteinase-9 gene expression by IFN-gamma and IFN-beta: critical role of STAT-1alpha. J. Immunol. *167*, 5150–5159.

Matthews, J.R., Sansom, O.J., and Clarke, A.R. (2011). Absolute requirement for STAT3 function in small-intestine crypt stem cell survival. Cell Death Differ. *18*, 1934–1943.

McCafferty, D.M., Mudgett, J.S., Swain, M.G., and Kubes, P. (1997). Inducible nitric oxide synthase plays a critical role in resolving intestinal inflammation. Gastroenterology *112*, 1022–1027.

Montgomery, R.K., Carlone, D.L., Richmond, C.A., Farilla, L., Kranendonk, M.E., Henderson, D.E., Baffour-Awuah, N.Y., Ambruzs, D.M., Fogli, L.K., Algra, S., et al. (2011). Mouse telomerase reverse transcriptase (mTert) expression marks slowly cycling intestinal stem cells. Proc. Natl. Acad. Sci. USA *108*, 179–184.

Musch, M.W., Clarke, L.L., Mamah, D., Gawenis, L.R., Zhang, Z., Ellsworth, W., Shalowitz, D., Mittal, N., Efthimiou, P., Alnadjim, Z., et al. (2002). T cell activation causes diarrhea by increasing intestinal permeability and inhibiting epithelial Na+/K+-ATPase. J. Clin. Invest. *110*, 1739–1747.

Neurath, M.F. (2014). New targets for mucosal healing and therapy in inflammatory bowel diseases. Mucosal Immunol. *7*, 6–19.

Pitsouli, C., Apidianakis, Y., and Perrimon, N. (2009). Homeostasis in infected epithelia: stem cells take the lead. Cell Host Microbe *6*, 301–307.

Radojevic, N., McKay, D.M., Merger, M., Vallance, B.A., Collins, S.M., and Croitoru, K. (1999). Characterization of enteric functional changes evoked by in vivo anti-CD3 T cell activation. Am. J. Physiol. *276*, R715–R723.

Rauch, I., Müller, M., and Decker, T. (2013). The regulation of inflammation by interferons and their STATs. JAKSTAT *2*, e23820.

Richmond, C.A., Shah, M.S., Deary, L.T., Trotier, D.C., Thomas, H., Ambruzs, D.M., Jiang, L., Whiles, B.B., Rickner, H.D., Montgomery, R.K., et al. (2015). Dormant intestinal stem cells are regulated by PTEN and nutritional status. Cell Rep. *13*, 2403–2411.

Robinson, S.P., Langan-Fahey, S.M., Johnson, D.A., and Jordan, V.C. (1991). Metabolites, pharmacodynamics, and pharmacokinetics of

tamoxifen in rats and mice compared to the breast cancer patient. Drug Metab. Dispos. *19*, 36–43.

Sandborn, W.J., Ghosh, S., Panes, J., Vranic, I., Wang, W., and Niezychowski, W.; Study A3921043 Investigators (2014). A phase 2 study of tofacitinib, an oral Janus kinase inhibitor, in patients with Crohn's disease. Clin. Gastroenterol. Hepatol. *12*, 1485–1493.e2.

Sato, T., Vries, R.G., Snippert, H.J., van de Wetering, M., Barker, N., Stange, D.E., van Es, J.H., Abo, A., Kujala, P., Peters, P.J., et al. (2009). Single Lgr5 stem cells build crypt-villus structures in vitro without a mesenchymal niche. Nature *459*, 262–265.

Srinivasan, T., Than, E.B., Bu, P., Tung, K.L., Chen, K.Y., Augenlicht, L., Lipkin, S.M., and Shen, X. (2016). Notch signalling regulates asymmetric division and inter-conversion between lgr5 and bmi1 expressing intestinal stem cells. Sci. Rep. *6*, 26069.

Stadnyk, A.W. (1994). Cytokine production by epithelial cells. FASEB J. *8*, 1041–1047.

Stempelj, M., Kedinger, M., Augenlicht, L., and Klampfer, L. (2007). Essential role of the JAK/STAT-1 signaling pathway in the expression of inducible nitric-oxide synthase in intestinal epithelial cells and its regulation by butyrate. J. Biol. Chem. *282*, 9797–9804.

Sturm, A., and Dignass, A.U. (2008). Epithelial restitution and wound healing in inflammatory bowel disease. World J. Gastroenterol. *14*, 348–353.

Takeda, N., Jain, R., LeBoeuf, M.R., Wang, Q., Lu, M.M., and Epstein, J.A. (2011). Interconversion between intestinal stem cell populations in distinct niches. Science *334*, 1420–1424.

Tian, H., Biehs, B., Warming, S., Leong, K.G., Rangell, L., Klein, O.D., and de Sauvage, F.J. (2011). A reserve stem cell population in small intestine renders Lgr5-positive cells dispensable. Nature *478*, 255–259.

Vermeire, K., Heremans, H., Vandeputte, M., Huang, S., Billiau, A., and Matthys, P. (1997). Accelerated collagen-induced arthritis in IFN-gamma receptor-deficient mice. J. Immunol. *158*, 5507–5513.

Wittkopf, N., Neurath, M.F., and Becker, C. (2014). Immune-epithelial crosstalk at the intestinal surface. J. Gastroenterol. *49*, 375–387.

Zhou, F., Rasmussen, A., Lee, S., and Agaisse, H. (2013). The UPD3 cytokine couples environmental challenge and intestinal stem cell division through modulation of JAK/STAT signaling in the stem cell microenvironment. Dev. Biol. *373*, 383–393.